



UCLA

NGA-Subduction Regional Ground Motion Models for Interface and Intraslab Events

Grace Parker, Jonathan Stewart, Behzad Hassani, Gail Atkinson and David Boore

PEER Annual Meeting
January 18, 2019

NGA-Subduction

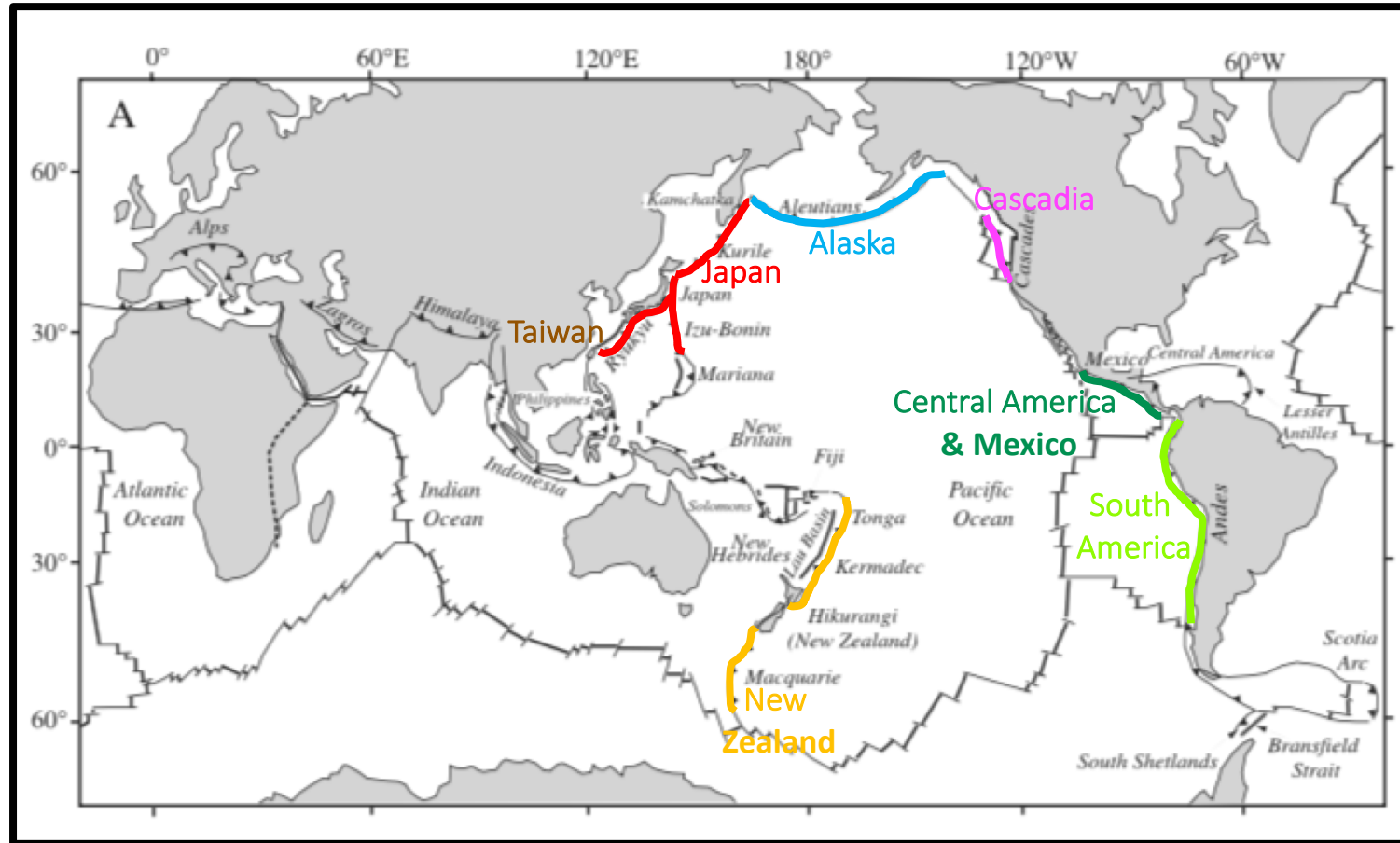


Figure 1a from Stern (2002) showing a map of global plate boundaries, with a focus on convergent locations

Subduction Zone Terminology

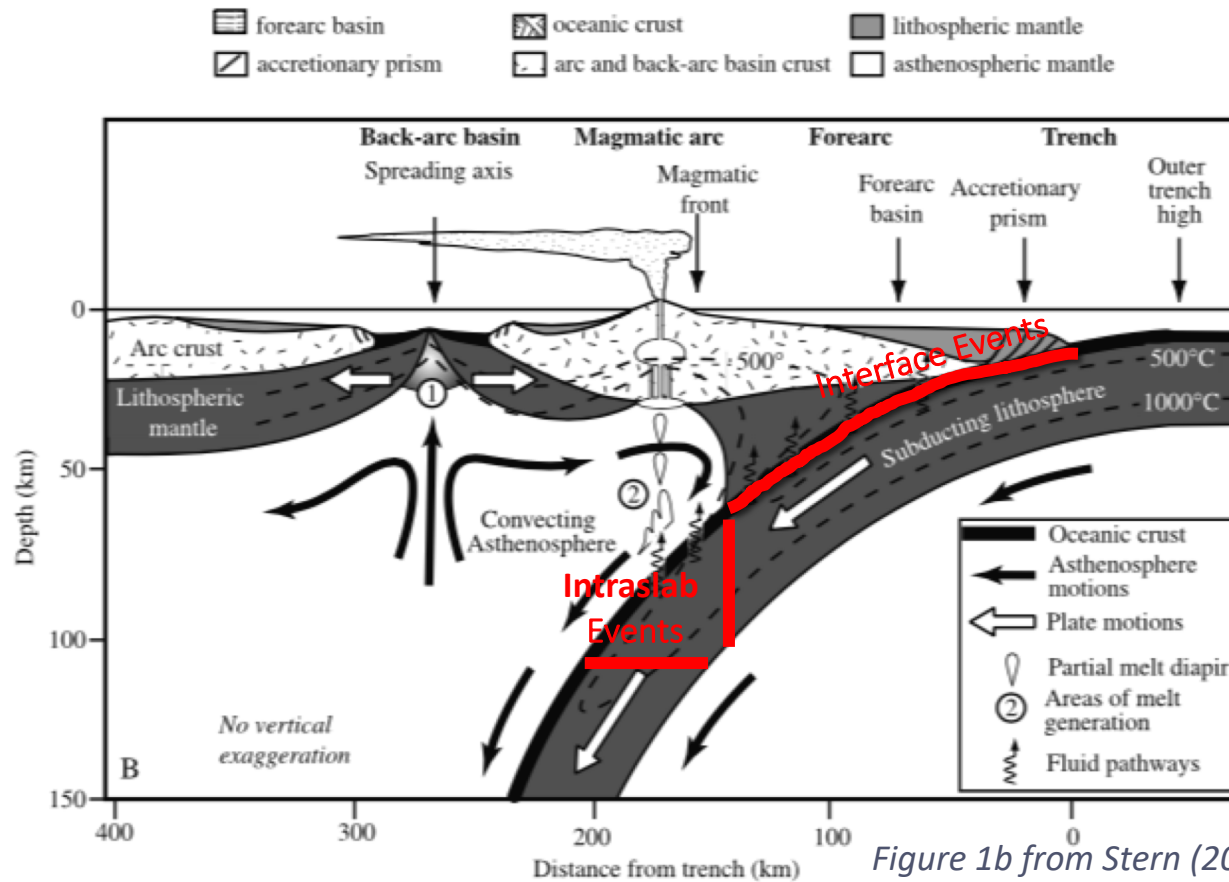
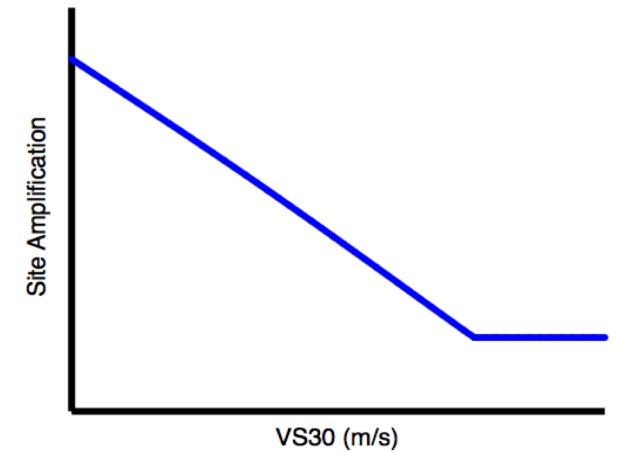


Figure 1b from Stern (2002) showing a schematic section through the upper 150km of a subduction zone

Model Development Approach

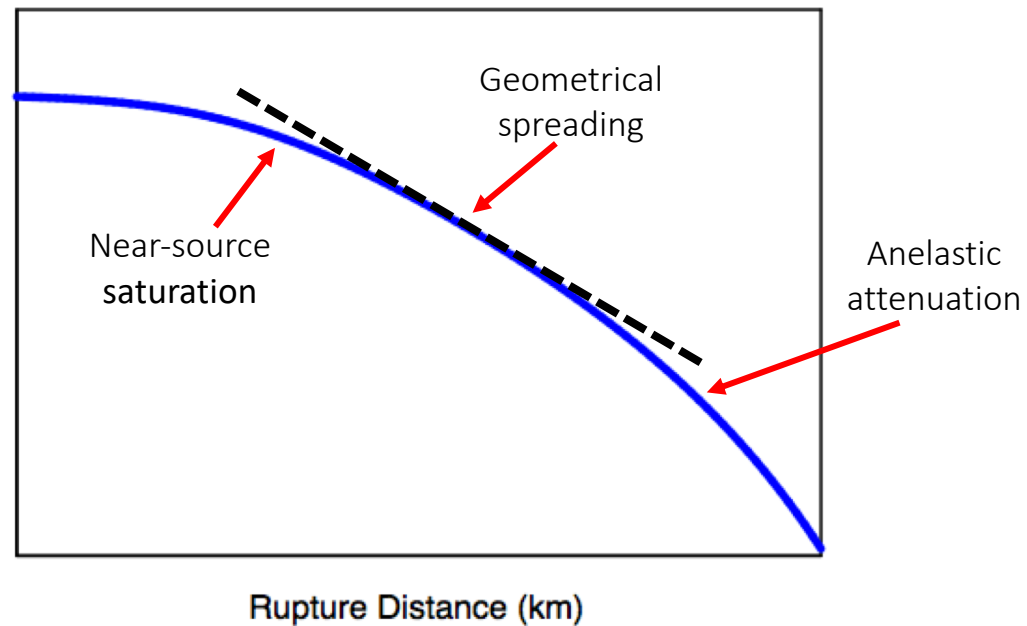
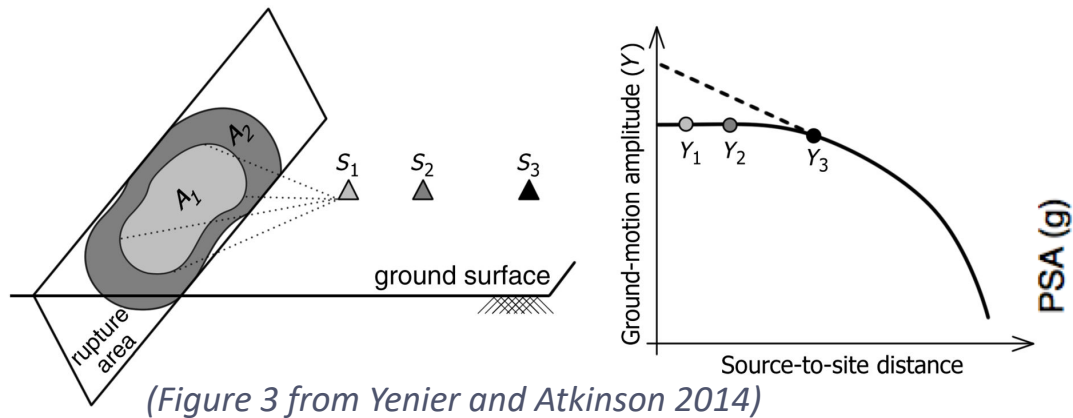
$$\mu_{ij} = F_{E,i} + F_{P,ij} + F_{S,j}$$

Use Seyhan and Stewart
(2014) to correct to 760 m/s



Model Development Approach

$$\mu_{ij} = F_{E,i} + F_{P,ij} + F_{S,j}$$



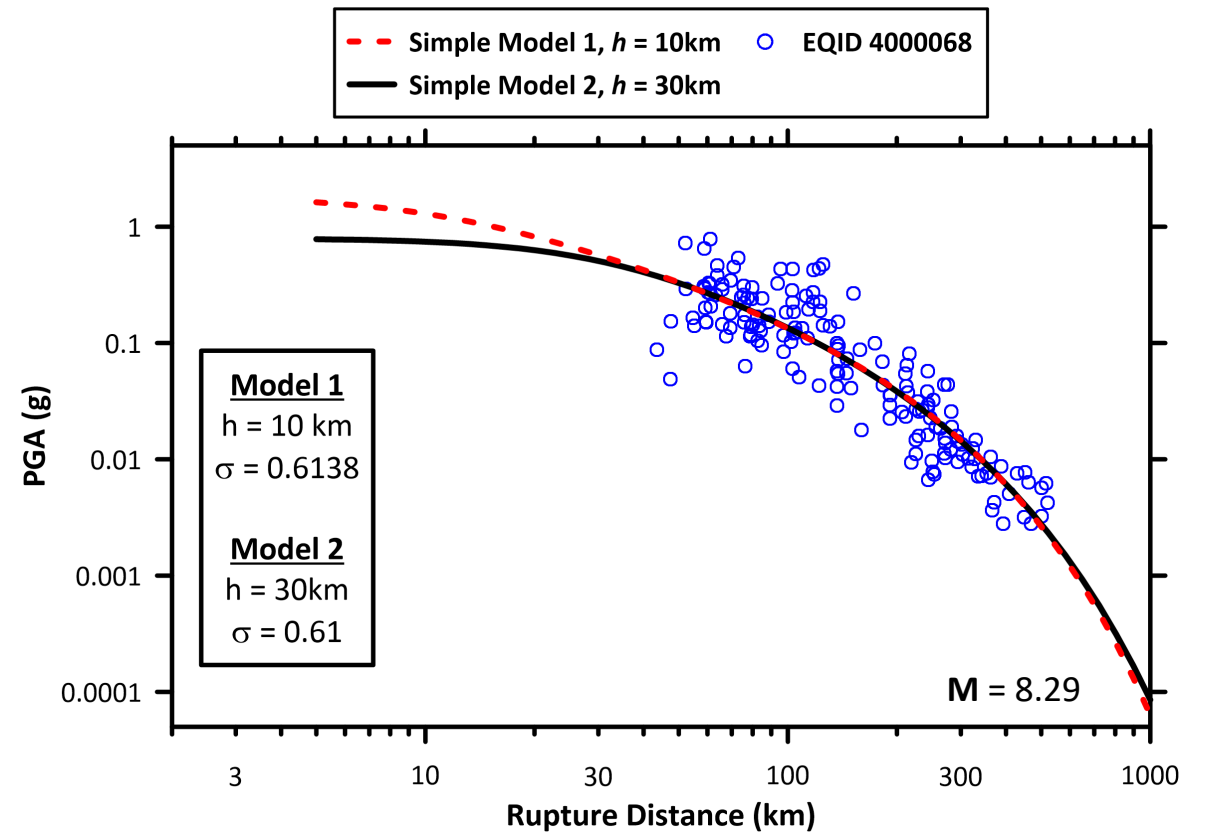
Model Development Approach

$$\mu_{ij} = F_{E,i} + F_{P,ij} + F_{S,j}$$

Use binning to deal with source term during path term development, then fit source model to residuals computed using completed path model. This term includes magnitude scaling and source depth scaling.

Near Source Saturation

- At small magnitudes, can constrain saturation empirically, using results from Atkinson et al. (2016), Yenier and Atkinson (2014)
- At large magnitudes, used EXSIM simulations
 - Source inputs based on NGA-Sub interface events
 - 5 events for each magnitude 4 – 9.5 with 0.25 steps
 - Dips 15-28°
 - Sites with azimuthal angles of 45,60, and 90° out to 1000km

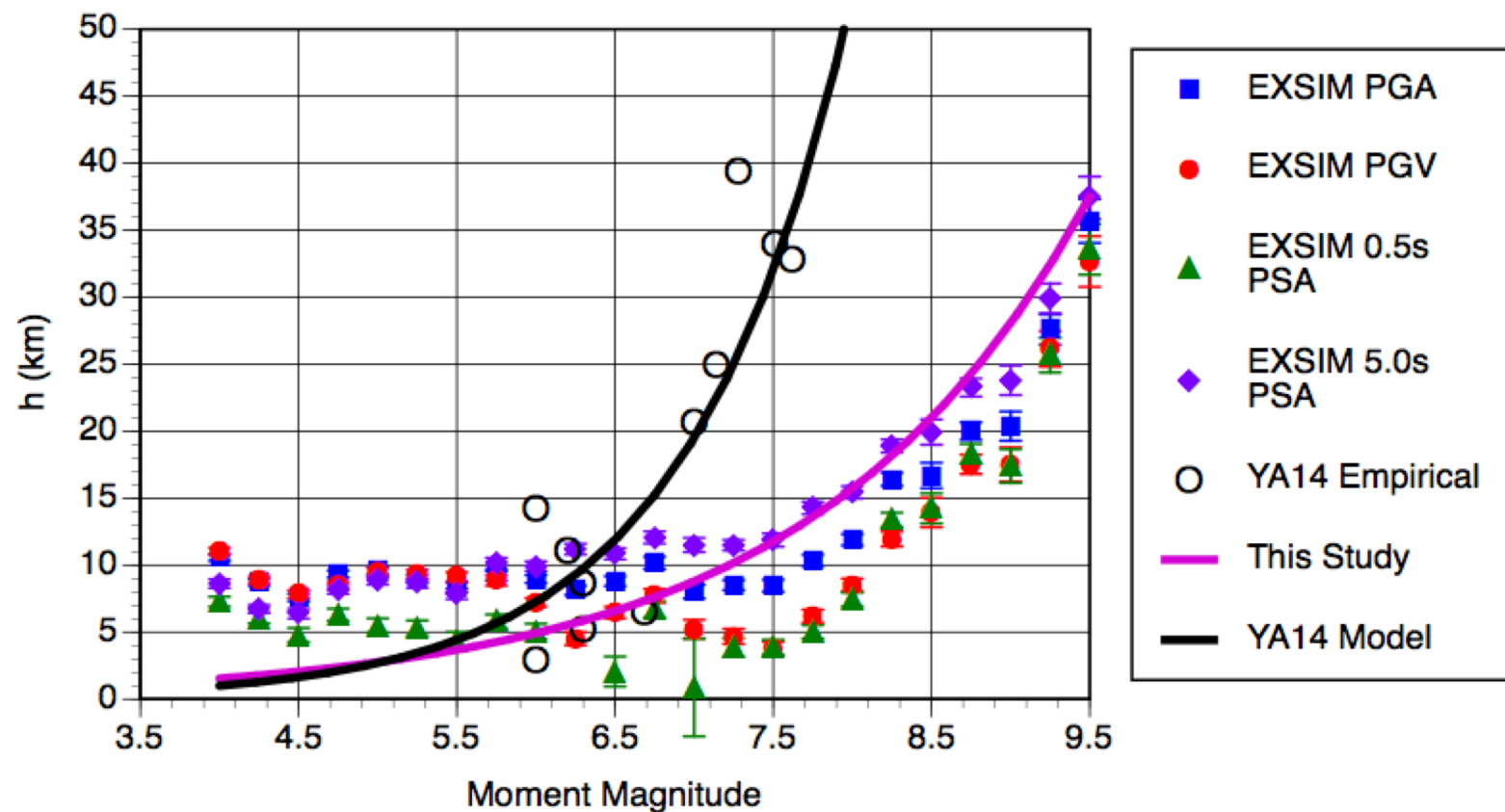


Near Source Saturation

$$F_P = f(R)$$

$$R = \sqrt{R_{Rup}^2 + h^2}$$

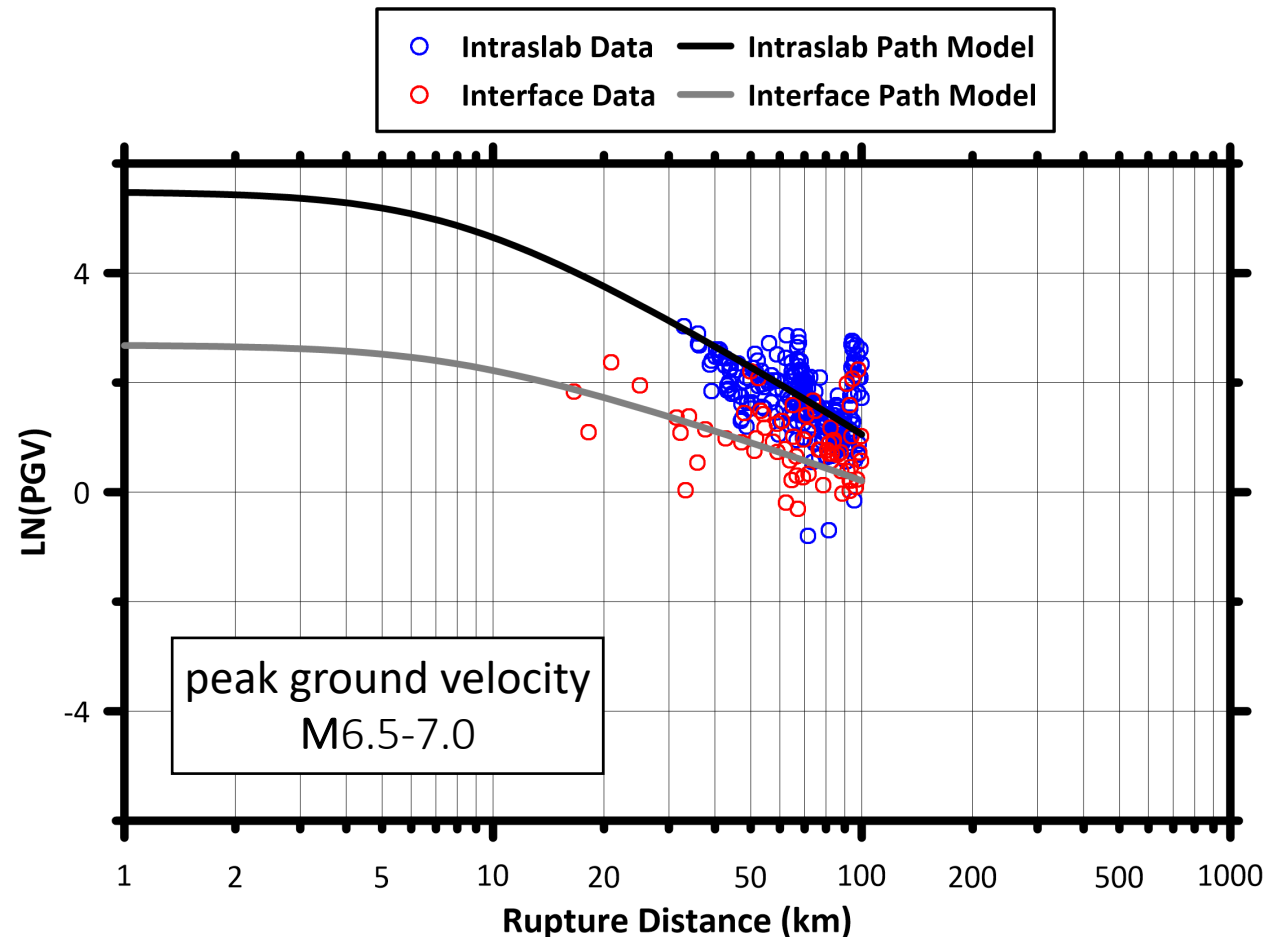
$$h = 10^{-0.82+0.252*M}$$



Semi-Empirical Geometric Spreading

$$F_{GS} = c_1 \ln R + (b_3 + b_4 M) \ln R$$

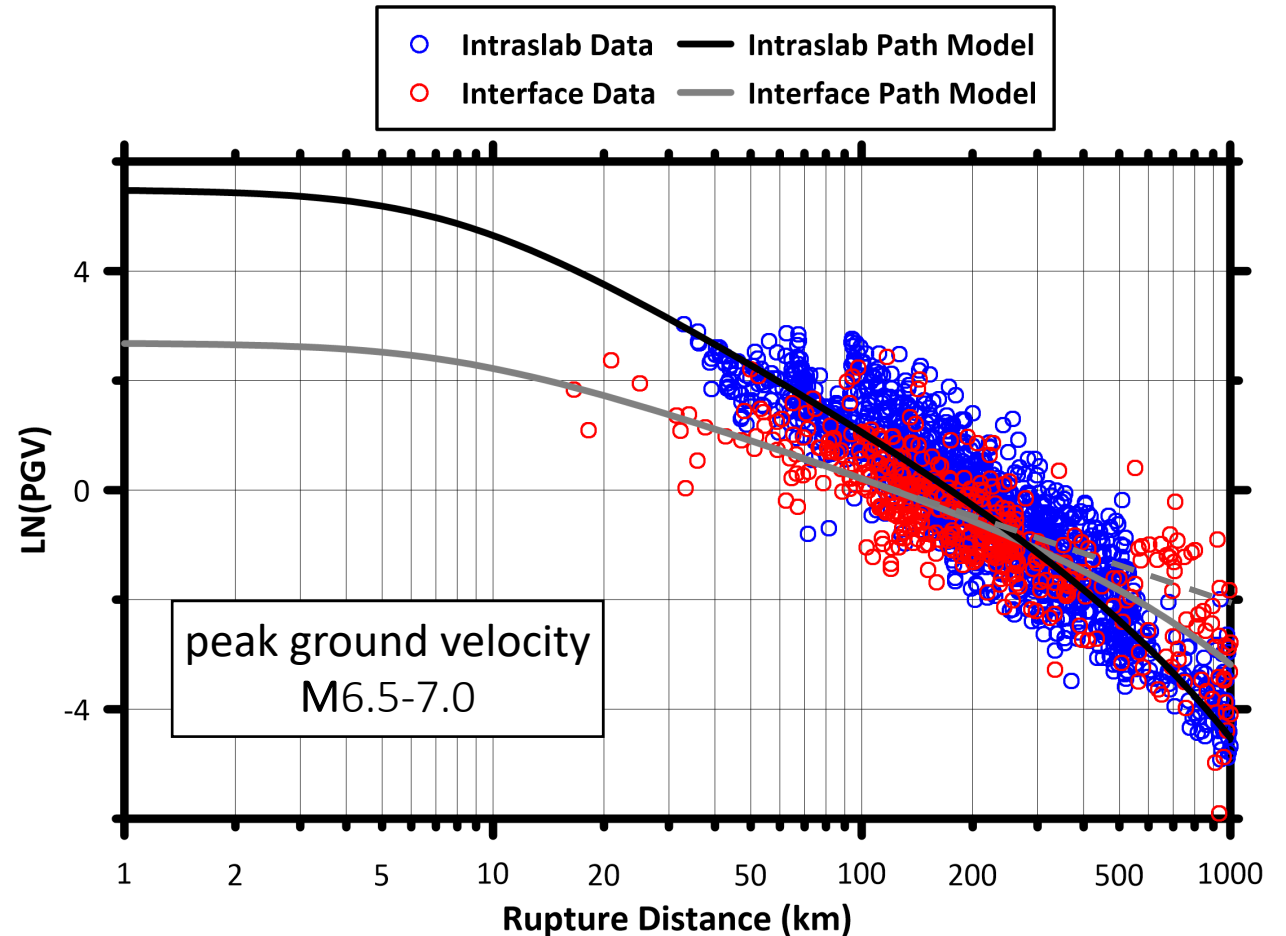
- Coefficient c_1 is set using data at $R_{rup} \leq 100\text{km}$, and is different for intraslab and interface events
- Magnitude dependence (b_4) set by Hassani and Atkinson (2018) simulations
- Earlier models assume same slope on R between event types (BC Hydro), or don't have M -dependence (Zea06, Atkinson and Macias 2009)



Global and Regional Anelastic

$$F_{AN} = a_0 R$$

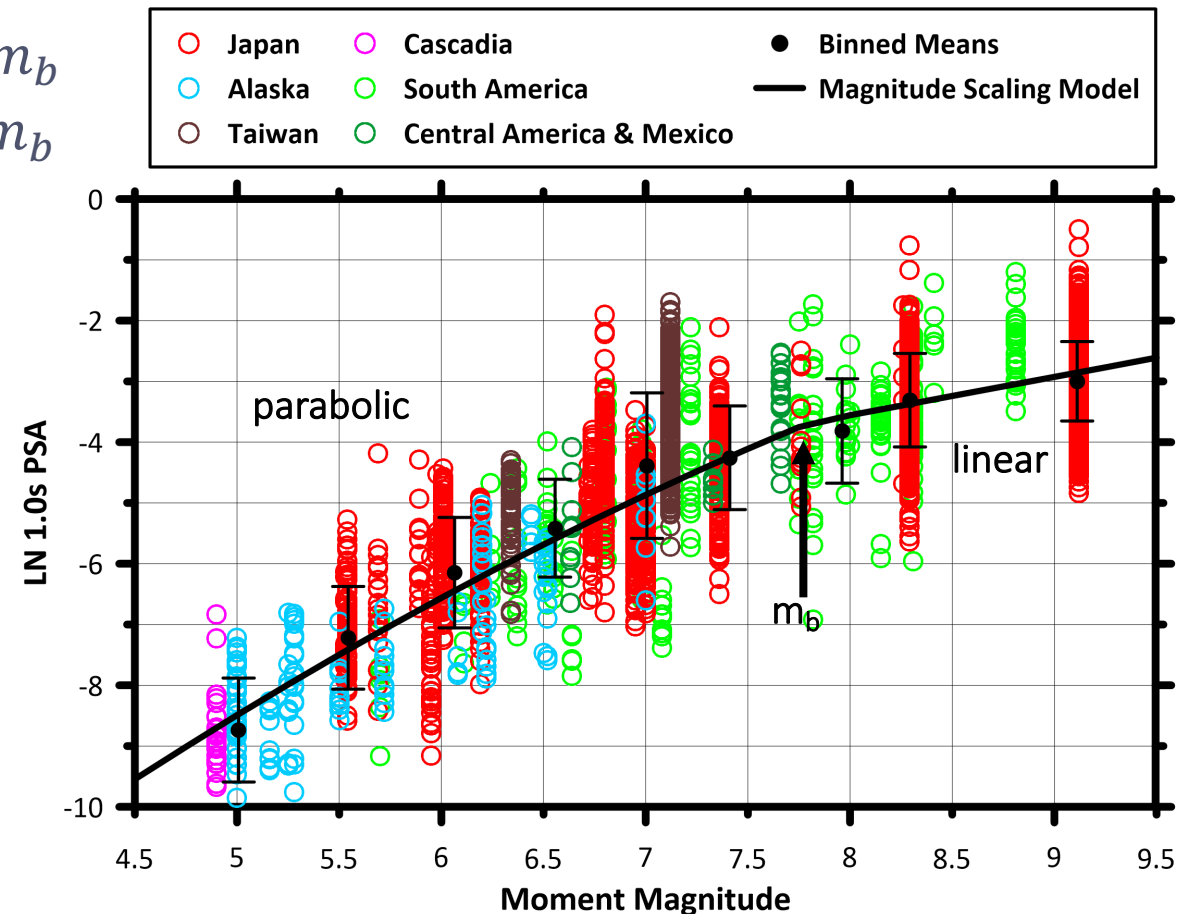
- Coefficient a_0 is determined empirically after GS term is set
- Interface and intraslab coefficients are different
- Coefficient a_0 is regionalized
- Global and regional values are regressed using mixed effects methods



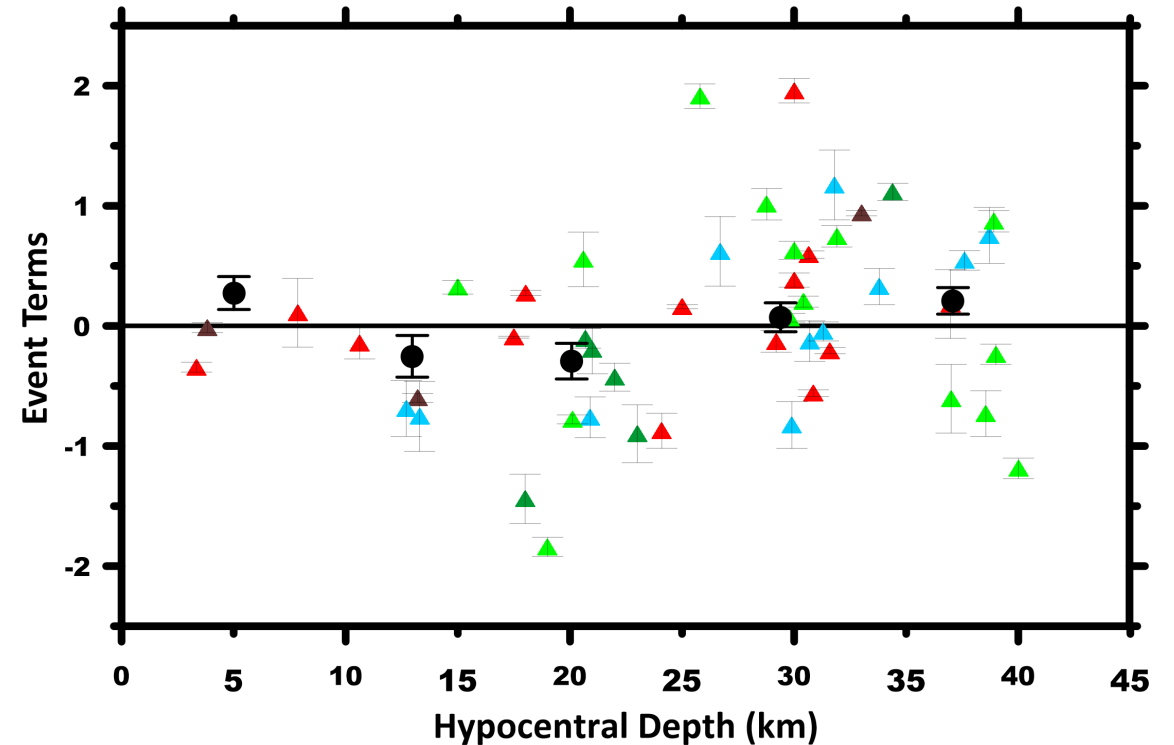
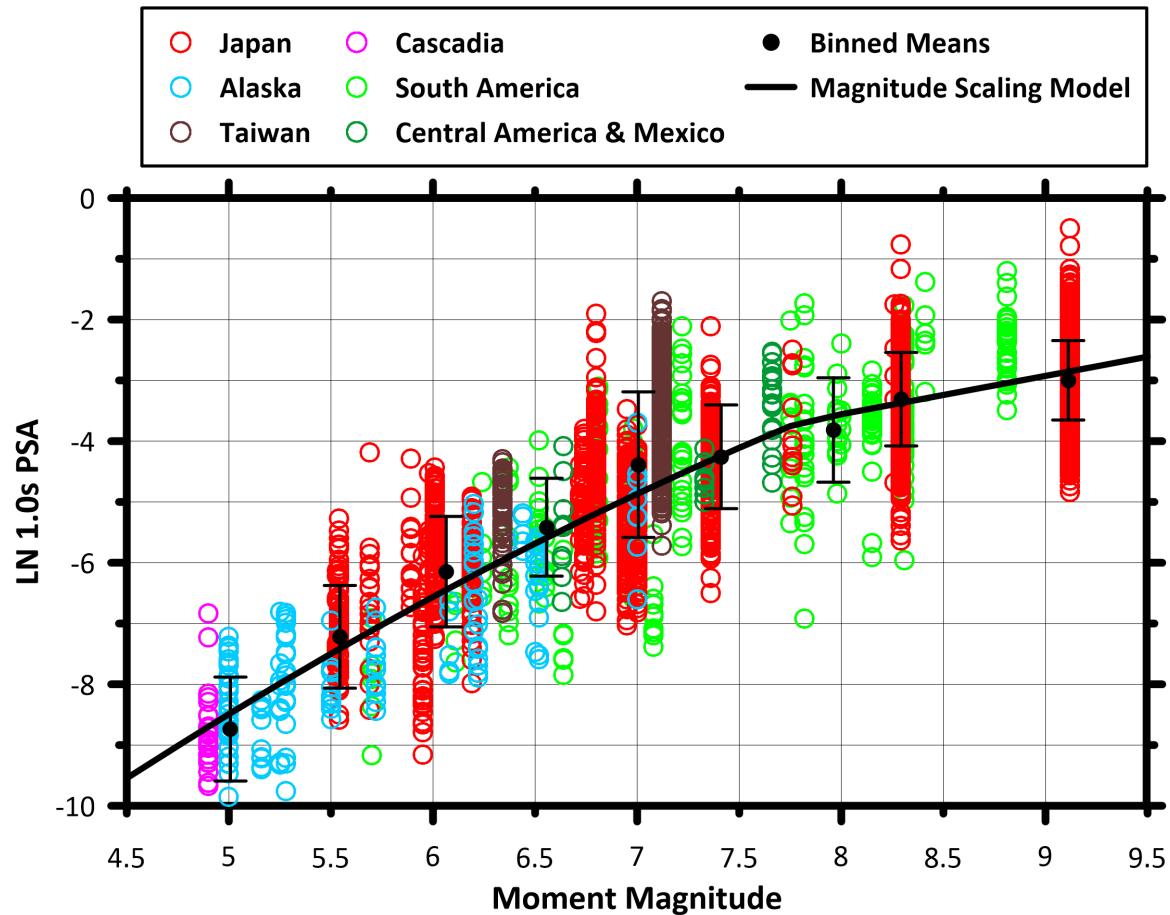
Magnitude Scaling Model

$$F_M = \begin{cases} c_0 + c_4(\mathbf{M} - m_b) + c_5(\mathbf{M} - m_b)^2 & \text{for } \mathbf{M} \leq m_b \\ c_0 + c_6(\mathbf{M} - m_b) & \text{for } \mathbf{M} > m_b \end{cases}$$

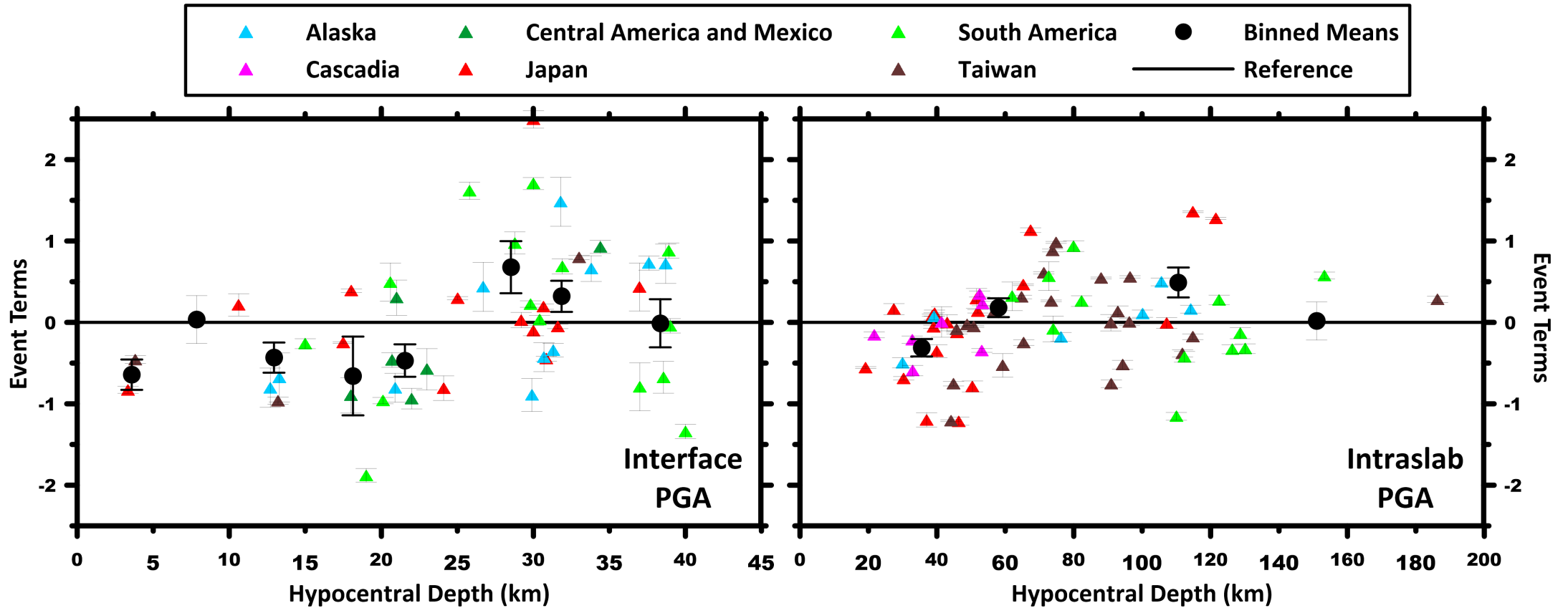
- Fit \mathbf{M} -scaling to residuals computed using completed path model
- Coefficients on \mathbf{M} empirical, with m_b from geometrical constraints (Archuleta and Ji 2018; Campbell 201x)
- m_b is regionalized



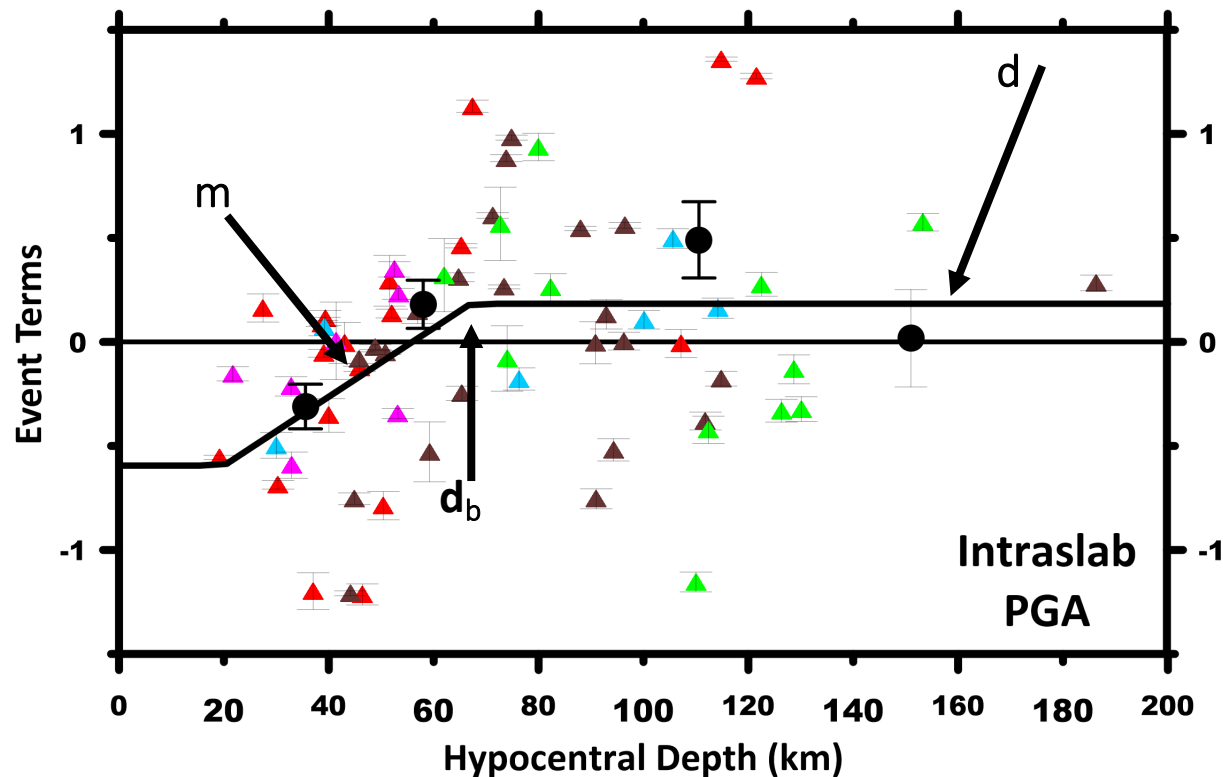
Source Depth Scaling



Source Depth Scaling



Source Depth Scaling



$$F_D = \begin{cases} m(d_{hyp} - d_b) + d & \text{for } d_{hyp} < d_b \\ d & \text{for } d_{hyp} \geq d_b \end{cases}$$

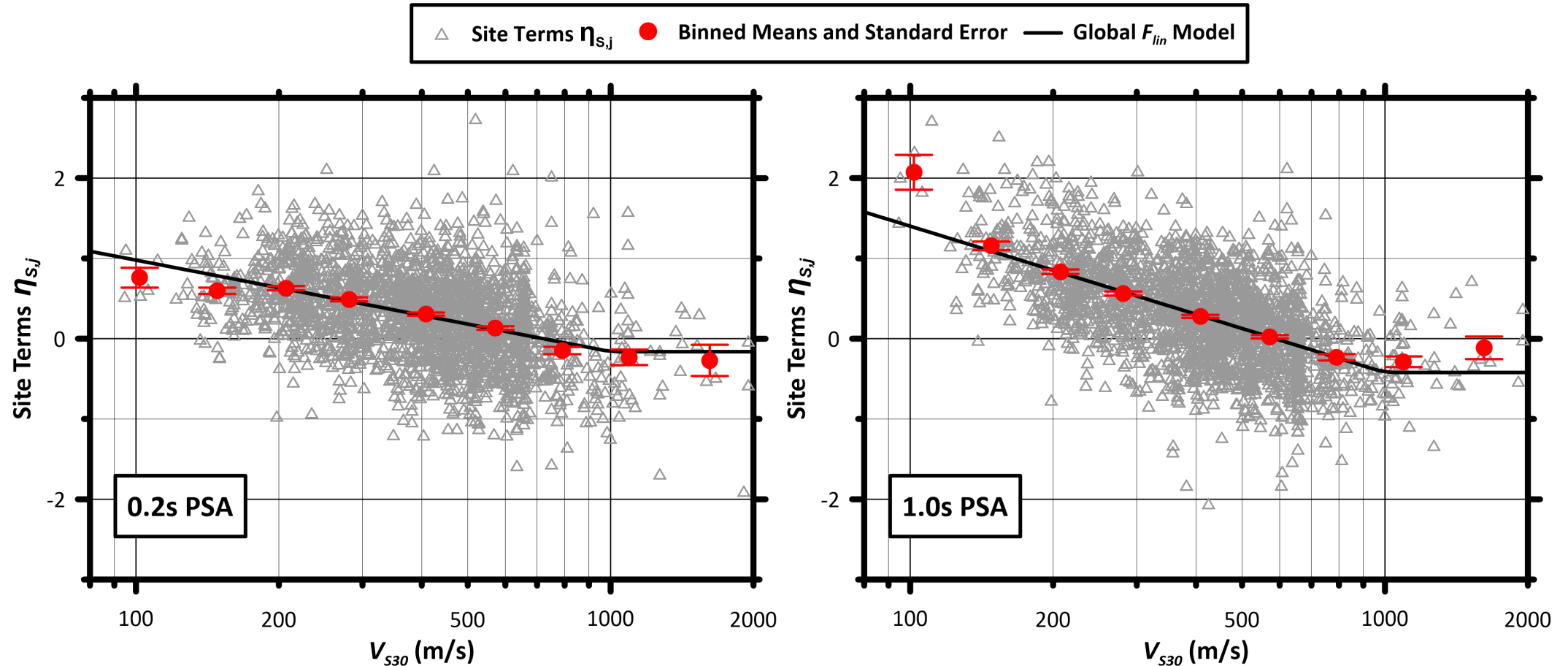
- Bi-linear model as a function of hypocentral depth
- Corner depth is period independent
- Model coefficients m , d , go to 0 at 2.0s for both even types

Linear Site Amplification

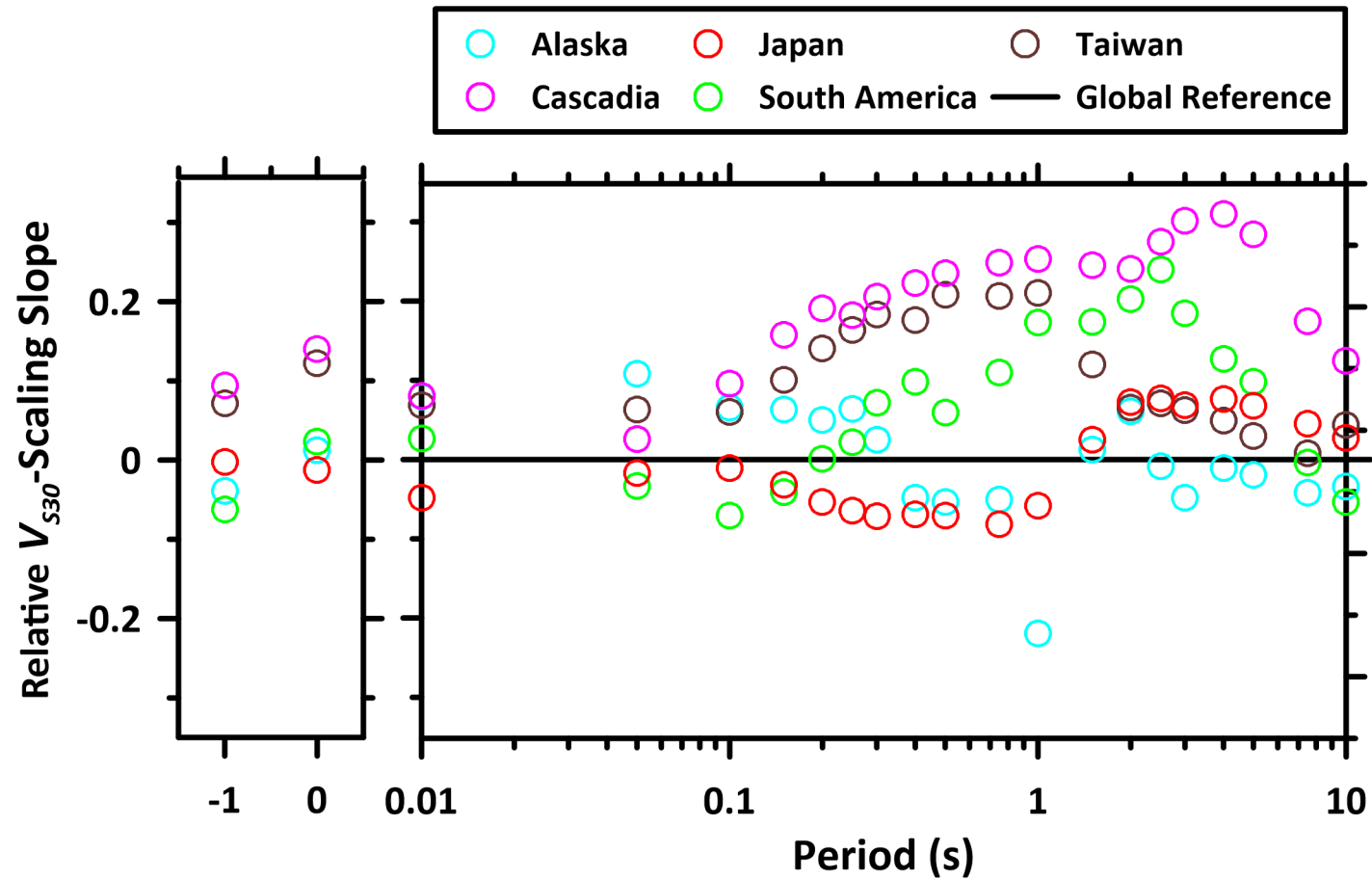
- Empirical site amplification computed using mixed effects analysis
- Within-event rock residuals computed utilizing the NGA-Sub GMM at 760m/s, associated event terms, and SS14 F_{nl} term
- Then use nonlinear least-squares to fit F_{lin} function

$$F_{lin} = \begin{cases} s_1 \ln\left(\frac{V_{S30}}{V_1}\right) + s_2 \ln\left(\frac{V_1}{V_{ref}}\right) & \text{for } V_{S30} \leq V_1 \\ s_2 \ln\left(\frac{V_{S30}}{V_{ref}}\right) & \text{for } V_1 < V_{S30} \leq V_2 \\ s_2 \ln\left(\frac{V_2}{V_{ref}}\right) & \text{for } V_{S30} > V_2 \end{cases}$$

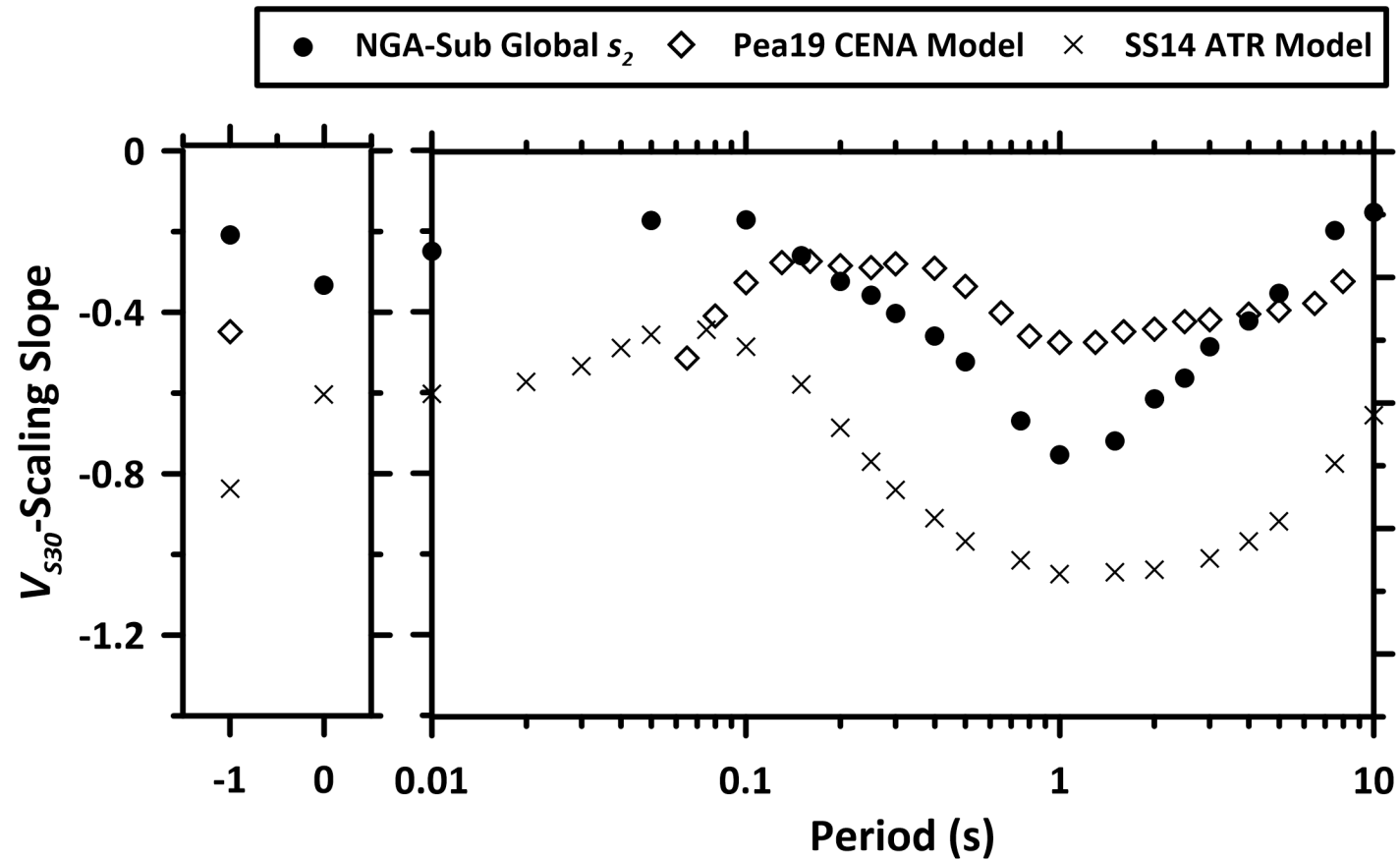
Global Linear Site Amplification



F_{lin} Slope Comparison



F_{lin} Slope Comparison



Ongoing Work

1. NGA-Subduction basin terms
2. NGA-Subduction GMM uncertainty model
3. Model verification; comparison of model to other NGA-Subduction models, and models from literature (e.g. Abrahamson et al. 2012; Atkinson and Boore 2003; Zhao et al. 2006; Zhao et al. 2016a,b)
4. Model validation against NGA-Subduction data from New Zealand, and Frankel et al. (2018) simulations for **M9** Cascadia interface events
5. Residuals analysis in regional back-arc regimes

Main Conclusions

- Developing a GMM for both interface and slab events, with regional constant, anelastic attenuation term, magnitude break point, and linear site term
- Model is semi-empirical; multiple elements constrained by simulations and geometry
 - Near-source saturation at large magnitudes
 - Magnitude dependent geometrical spreading
 - Magnitude break-point, m_b
- Site response term is subduction-specific and regional:
 - Regional V_{s30} – scaling
 - NGA-Sub nonlinear site amplification model
 - Ongoing work is evaluating regional basin effects (Japan, Seattle, Taipei)

References

- Abrahamson, N.A., Kuehn, N., Gulerce, Z., Gregor, N., Bozorgnia, Y., Parker, G.A., Stewart, J.P., Chiou, B., Idriss, I.M., Campbell, K.W., and Youngs, R. (2018). Update of the BC Hydro Subduction Ground-Motion Model using the NGA- Subduction Dataset. *PEER Report 2018/02*. PEER, Berkeley, CA.
- Abrahamson, N., Gregor, N. and Addo, K. (2016). BC Hydro ground motion prediction equations for subduction earthquakes. *Earthq. Spectra*, **32**, 23-44.
- Atkinson, G.M. and Boore, D.M. (2003). Empirical ground-motion relations for subduction-zone earthquakes and their application to Cascadia and other regions. *Bull. Seismol. Soc. Am.*, **93**, 1703-1729.
- Atkinson, G.M., Yenier, E., Sharma, N. and Convertito, V. (2016). Constraints on Near-Distance Saturation of Ground Motion Amplitudes for Small-to-Moderate Induced Earthquakes. *Bull. Seismol. Soc. Am.* **106**, 2104-2111.
- Goulet, C.A., T. Kishida, T.D. Ancheta, C.H. Cramer, R.B. Darragh, W.J. Silva, Y.M.A. Hashash, J.A. Harmon, J.P. Stewart, K.E. Wooddell, and R.R. Youngs (2014). PEER NGA-East Database, *PEER Report 2014/17*, Pacific Earthquake Engineering Research Center, Berkeley, CA
- Hassani, B. and Atkinson, G.M. (2018). Adjustable Generic Ground-Motion Prediction Equation Based on Equivalent Point-Source Simulations: Accounting for Kappa Effects. *Bull. Seismol. Soc. Am.*, **108**, 913-928.
- Parker, G.A., J.P. Stewart, Y.M.A. Hashash, E.M. Rathje, K.W. Campbell, and W.J. Silva (2019). Empirical Linear Seismic Site Amplification in Central and Eastern North America. *Earthq. Spectra*, *preprint*.
- Seyhan, E., and Stewart, J. P. (2014). Semi-empirical nonlinear site amplification from NGA-West2 data and simulations. *Earthq. Spectra*, **30**, 1241-1256.
- Stern, R.J. (2002). Subduction zones. *Rev. Geophys.*, **40**, 1012.
- Sharma, N., Convertito, V., Maercklin, N. and Zollo, A. (2013). Ground-motion prediction equations for the Geysers geothermal area based on induced seismicity records. *Bull. Seismol. Soc. Am.*, **103**, 117-130.
- Yenier, E. and Atkinson, G.M. (2014). Equivalent point-source modeling of moderate-to-large magnitude earthquakes and associated ground-motion saturation effects. *Bull. Seismol. Soc. Am.*, **104**, 1458-1478.
- Zhao, J.X., Liang, X., Jiang, F., Xing, H., Zhu, M., Hou, R., Zhang, Y., Lan, X., Rhoades, D.A., Irikura, K. and Fukushima, Y. (2016). Ground-motion prediction equations for subduction interface earthquakes in Japan using site class and simple geometric attenuation functions. *Bull. Seismol. Soc. Am.* **106**, 1518-1534.
- Zhao, J.X., Jiang, F., Shi, P., Xing, H., Huang, H., Hou, R., Zhang, Y., Yu, P., Lan, X., Rhoades, D.A. and Somerville, P.G. (2016). Ground-motion prediction equations for subduction slab earthquakes in Japan using site class and simple geometric attenuation functions. *Bull. Seismol. Soc. Am.* **106**, 1535-1551.
- Zhao, J.X., Zhang, J., Asano, A., Ohno, Y., Oouchi, T., Takahashi, T., Ogawa, H., Irikura, K., Thio, H.K., Somerville, P.G. and Fukushima, Y. (2006). Attenuation relations of strong ground motion in Japan using site classification based on predominant period. *Bull. Seismol. Soc. Am.*, **96**, 898-913.